

Detailed Analysis of p+p Elastic Scattering Data in the Quark-Diquark Model of
Bialas and Bzdak
from $\sqrt{s} = 23.5$ GeV to 7 TeV

F. Nemes

*Institute of Physics, Eötvös University
Pázmány P. s. 1/A, H-1117 Budapest, Hungary**

T. Csörgő

*Wigner Research Centre for Physics, RMKI
H-1525 Budapest 114, P.O.Box 49, Hungary†*

Final results of a detailed analysis of p+p elastic scattering data are presented, utilizing the quark-diquark model of protons in a form proposed by Bialas and Bzdak. The differential cross-section of elastic proton-proton collisions is analyzed in a detailed and systematic manner at small momentum transfers, starting from the energy range of CERN ISR at $\sqrt{s} = 23.5$ GeV, including also recent TOTEM data at the present LHC energies at $\sqrt{s} = 7$ TeV. These studies confirm the picture that the size of proton increases systematically with increasing energies, while the size of the constituent quarks and diquarks remains approximately independent of (or only increases only slightly with) the colliding energy. The detailed analysis indicates correlations between model parameters and also indicates an increasing role of shadowing at LHC energies. Within the investigated class of models, a simple and model-independent phenomenological relation was discovered that connects the total p+p scattering cross-section to the effective quark, diquark size and their average separation. Our best fits indicate, that the relative error of this phenomenological relation is 10-15 % in the considered energy range.

arXiv:1204.5617v2 [hep-ph] 1 Sep 2012

* frigyes.janos.nemes@cern.ch

† csorgo.tamas@wigner.mta.hu

I. INTRODUCTION

The differential cross section of elastic scattering of p+p collisions allows one to study the internal structure of protons using the theory of diffraction. Varying the momentum transfer one can change the resolution of the investigation: increasing the momentum transfer corresponds to looking more and more deeply inside the structure of protons. One of the fundamental outcomes of diffractive p+p scattering studies was the indication that protons have a finite size and a complicated internal structure, thus the protons can be considered as composite objects.

Our interest in this problem has been triggered by two factors: an interesting series of recent theoretical work and also new data from the TOTEM experiment at CERN LHC. These are detailed below.

Recently, we became aware of an inspiring series of papers of Bialas, Bzdak and collaborators, who studied elastic proton-proton [1], pion-proton [2] and nucleus-nucleus collisions [3, 4] in a framework where the proton was considered as a composite object that contains correlated quark and diquark constituents. In this work, we confirm their main conclusion: the quark-diquark model of nucleon structure at low momentum transfer does capture the main features of this problem and indeed it deserves a closer, more detailed attention. The first results that form the basis of our current study were made public in a proceeding material [5]. In that study we already reported about several details of the present investigation. In contrast to the paper of Bialas and Bzdak in ref. [1], we not only included an estimation of the best values of the model parameters, but also determined their errors and also the fit quality.

In this paper, we refined our first results [5] by decreasing the number of fit parameters from five to three which leads to a far better error estimation, and less correlations among the remaining three model parameters. In order to reach these goals, we utilized standard experimental techniques, such as multi-parameter optimization or fitting with the help of the MINUIT function minimalization and multi-parameter optimization package [6].

In addition to these simple, straightforward and interesting theoretical investigations of elastic scattering data from CERN ISR in the energy range of $\sqrt{s} = 23.5, 30.7, 52.9$ and 62.5 GeV, that were already analyzed in ref. [1], new elastic scattering data became available recently at $\sqrt{s} = 7$ TeV [7] from the CERN LHC experiment TOTEM. The new data triggered a wide spectrum of theoretical investigations, including Regge theory based studies [8–11] involving perturbative QCD(BFKL) [12], as well as study with hidden dimensions [13]. Extrapolation to the domain of cosmic rays [14] become available. We have tested both variations of the model of Bialas and Bzdak of ref. [1], not only at ISR energies but also at the currently available highest LHC energies on recent TOTEM data, in order to learn more details about the evolution of the properties of p+p elastic interactions in the recently opened, few TeV energy range. The two variations of the Bialas and Bzdak model allowed us to obtain an effective radius parameter R_{eff} which is model independent within errors. A simple relation between the total cross section and the effective radius is also presented in the discussions.

Most of the arguments for the composite structure of hadrons have been derived from the studies of lepton-hadron interactions. The standard picture is that hadrons are either mesons, composed of valence quarks and anti-quarks, or (anti)baryons, composed of three valence (anti)quarks, that carry the quantum numbers, while the electrically neutral gluons carry color charges and provide the binding among the quarks and anti-quarks. The exact contribution of quarks, gluons, and the sea of virtual quark-antiquark pairs and gluons to certain hadronic properties e.g. spin is still under detailed investigation. Also, more than 10 exotic hadronic resonances called X, Y and Z states were recently discovered in electron-positron collisions at the world's highest luminosities in the BELLE experiment at KEK. These hadronic states cannot be interpreted in the standard picture of quark-antiquark or three (anti)quark bound states, according to refs. [15, 16]. Thus even nowadays there are still several open questions that are related to the compositeness of the hadrons in general. As gluons do not interact directly with leptons, their properties are best explored with the help of the strong hadronic interactions. For example, the gluon contribution to the proton spin is investigated with the help of polarized proton - polarized proton collisions at RHIC [17], but it is still not fully constrained. In this work, we focus on the effects of internal correlations between the quarks inside the protons, reporting on a detailed study of proton-proton elastic scattering at several ISR and also at the currently top available LHC energies. Let us recall, that a similar analysis involving three *independent* quarks was not able to properly describe the ISR data [18]. In that model quarks were considered as “dressed” valence quarks in the sense that they contain the gluonic and $q\bar{q}$ contribution as well, as if the glue would be concentrated around pointlike valence quarks. Thirty-five years after the three independent quark model of ref. [18] another three-quark model of the protons was proposed in ref. [1], that included interesting correlations between two dressed valence quarks to form a diquark. In the present investigation this quark-diquark model [1], is compared to data in details.

The quark-diquark picture of elastic p+p scattering is similar to the Glauber optical model [19] in nuclear physics. This Glauber model, developed originally for nuclear multiple scattering problems like cross sections of protons and neutrons on deuteron, became a standard model of high energy interactions in nuclear physics where multiple interactions are built up from superpositions of nucleon-nucleon scattering. This model became a fundamental and successful tool in describing nuclear collisions at high energy [20].

The body of this manuscript is organized as follows: the theoretical model of Bialas and Bzdak is recapitulated and

summarized in Section II, including two cases. In the first case, the proton is modelled as a quark-diquark composite system, while in the second case, the diquark is assumed to have a quark-quark internal structure. Section III contains our final results, which is based on a multiparameter optimization procedure, utilizing the CERN MINUIT package [6]. Finally, we summarize and conclude in Section IV.

II. ELASTIC SCATTERING IN THE QUARK-DIQUARK MODEL

We describe proton-proton interactions as collision of two systems, each one composed of a dressed quark and diquark. The p+p collision is schematically illustrated on Fig. 1.

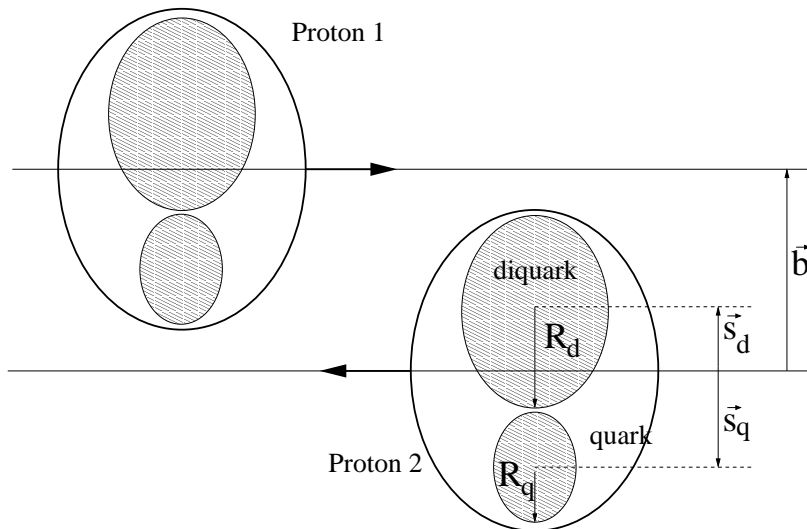


FIG. 1. Scheme of the scattering of two protons, when the proton is assumed to have a quark-diquark structure and the diquark is assumed to be scattered as a single entity. This is just a snapshot and all the model parameters follow a Gaussian distribution. Note, that a center of mass energy dependent Lorentz-contraction determines the longitudinal scale parameters.

The interaction between quarks and diquarks is assumed to be purely absorptive. Consequently the amplitude has no real part and the imaginary part – dominating at high energy – is given by the absorption of the incoming particle wave, represented by the inelastic (non-diffractive) collisions.

In the impact parameter space the inelastic proton-proton cross-section for a fixed impact parameter \vec{b} can be given by the following formula [1]

$$\sigma(\vec{b}) = \int_{-\infty}^{+\infty} \dots \int_{-\infty}^{+\infty} d^2 s_q d^2 s'_q d^2 s_d d^2 s'_d D(\vec{s}_q, \vec{s}_d) D(\vec{s}'_q, \vec{s}'_d) \sigma(\vec{s}_q, \vec{s}_d; \vec{s}'_q, \vec{s}'_d; \vec{b}), \quad (1)$$

where \vec{s}_q , \vec{s}'_q and \vec{s}_d , \vec{s}'_d are the transverse positions of the quarks and diquarks respectively. The integrand is a product of quark-diquark distributions of the incoming protons and a σ function which gives the probability of inelastic interaction at given impact parameter \vec{b} and at given quark, diquark positions.

The quark-diquark distribution inside the nucleon is taken into account with the following Gaussian

$$D(\vec{s}_q, \vec{s}_d) = \frac{1 + \lambda^2}{\pi R_{qd}^2} e^{-(s_q^2 + s_d^2)/R_{qd}^2} \delta^2(\vec{s}_d + \lambda \vec{s}_q), \quad \lambda = m_q/m_d, \quad (2)$$

where R_{qd} is the RMS of the separation between the CMS of the diquark and the remaining quark in the proton. λ is the mass ratio of the quark and the diquark. Obviously $1/2 \leq \lambda \leq 1$, where $1/2$ would indicate a loosely bound diquark. The two dimensional delta function fixes the position of the center of mass in the transverse plane.

Elastic interactions are *independent*, accordingly the probability distribution of elastic proton-proton collision is the *product* of the probability distribution of elastic interactions of their constituents [21, 22]

$$\sigma(\vec{s}_q, \vec{s}_d; \vec{s}'_q, \vec{s}'_d; \vec{b}) = 1 - \prod_{a,b \in \{q,d\}} \left[1 - \sigma_{ab}(\vec{b} + \vec{s}'_a - \vec{s}_b) \right]. \quad (3)$$

The inelastic differential cross-sections are parametrized with Gaussian distributions

$$\sigma_{ab}(\vec{s}) = A_{ab}e^{-s^2/R_{ab}^2}, \quad R_{ab}^2 = R_a^2 + R_b^2, \quad (4)$$

where R_{ab} is the variance of having an inelastic collision, which is calculated from the sum of the squared R_q, R_d radius parameters; the A_{ab} parameters are the amplitudes. From unitarity the elastic amplitude in impact parameter space

$$t_{el}(\vec{b}) = 1 - \sqrt{1 - \sigma(\vec{b})}. \quad (5)$$

As it was mentioned the real part of the amplitude is ignored. Recently, the important role of the real part of the elastic scattering amplitude in shaping $d\sigma/dt$ at the dip and in the Orear region was highlighted in [23, 24].

The elastic amplitude in momentum transfer representation is the Fourier-transform of the amplitude in impact parameter space

$$T(\vec{\Delta}) = \int_{-\infty}^{+\infty} \int_{-\infty}^{+\infty} t_{el}(\vec{b}) e^{i\vec{\Delta} \cdot \vec{b}} d^2b = 2\pi \int_0^{+\infty} t_{el}(b) J_0(\Delta b) b db, \quad (6)$$

where $\Delta = |\vec{\Delta}|$, $b = |\vec{b}|$ and J_0 is the zeroth Bessel-function of the first kind. Then the elastic differential cross section reads as

$$\frac{d\sigma}{dt} = \frac{1}{4\pi} |T(\Delta)|^2. \quad (7)$$

A. Model $p = (q, d)$: The diquark is assumed to scatter as a single entity

The subject of this section is to analyze, as the first investigated case, that variant of the model of Bialas and Bzdak, when the quark and the diquark is considered to scatter as one entity as indicated on Fig. 1. In this case, the number of free parameters can be reduced if we assume that the number of partons is twice as many in the diquark than in the quark. From the inelastic differential cross sections (4) the total inelastic cross sections are

$$\sigma_{ab} = \int_{-\infty}^{+\infty} \int_{-\infty}^{+\infty} \sigma_{ab}(\vec{s}) d^2s = \pi A_{ab} R_{ab}^2, \quad a, b \in \{q, d\}. \quad (8)$$

Our assumption tells us that

$$\sigma_{qq} : \sigma_{qd} : \sigma_{dd} = 1 : 2 : 4, \quad (9)$$

from which we can deduce the following expressions

$$A_{qd} = A_{qq} \frac{4R_q^2}{R_q^2 + R_d^2}, \quad A_{dd} = A_{qq} \frac{4R_q^2}{R_d^2}, \quad (10)$$

which means that every A_{ab} parameter can be expressed in term of A_{qq} . With these ingredients the calculation of each term in (1) reduces to Gaussian integrations. Two of the Dirac δ functions in (1) induce the following transformation in the transverse diquark and quark position variables

$$\vec{s}_d = -\lambda \vec{s}_q, \quad \vec{s}_d' = -\lambda \vec{s}_q'. \quad (11)$$

Hence four Gaussian integration remain, which lead us to the following result [1]

$$\begin{aligned} & \frac{4v^2}{\pi^2} \int_{-\infty}^{+\infty} \int_{-\infty}^{+\infty} d^2s_q d^2s_q' e^{-2v(s_q^2 + s_q'^2)} e^{-c_{qq}(b-s_q+s_q')^2} e^{-c_{qd}(b-s_q+s_d')^2} \\ & \times e^{-c_{dq}(b-s_d+s_q')^2} e^{-c_{dd}(b-s_d+s_d')^2} = \frac{4v^2}{\Omega} e^{-b^2 \frac{\Gamma}{\Omega}}, \end{aligned} \quad (12)$$

where the coefficients c_{ab} are abbreviations, and

$$\Omega = \left[4v + (1 + \lambda)^2 (c_{qd} + c_{dq}) \right] \left[v + c_{qq} + \lambda^2 c_{dd} \right] + (1 - \lambda)^2 \left[v (c_{qd} + c_{dq}) + (1 + \lambda)^2 c_{qd} c_{dq} \right], \quad (13)$$

while

$$\Gamma = \left[4v + (1 + \lambda)^2 (c_{qd} + c_{dq}) \right] \left[v (c_{qq} + c_{dd}) + (1 + \lambda)^2 c_{qq} c_{dd} \right] + \left[4v + (1 + \lambda)^2 (c_{qq} + c_{dd}) \right] \left[v (c_{qd} + c_{dq}) + (1 + \lambda)^2 c_{qd} c_{dq} \right]. \quad (14)$$

B. Model $p = (q, (q, q))$: The diquark is assumed to scatter as a composite object

When the diquark is assumed to scatter as a composite object, that includes two valence quarks, the scheme of elastic p+p scattering is illustrated on Fig. 2. Following Bialas and Bzdak [1], the quark distribution inside the diquark is supposed to have the following Gaussian shape

$$D(\vec{s}_{q1}, \vec{s}_{q2}) = \frac{1}{\pi d^2} e^{-(s_{q1}^2 + s_{q2}^2)/2d^2} \delta^2(\vec{s}_{q1} + \vec{s}_{q2}), \quad (15)$$

where \vec{s}_{q1} and \vec{s}_{q2} are the transverse quark positions inside the diquark, and

$$d^2 = R_d^2 - R_q^2 \quad (16)$$

is the RMS of the separation of quarks inside the diquark, calculated from the diquark and quark radius parameters.

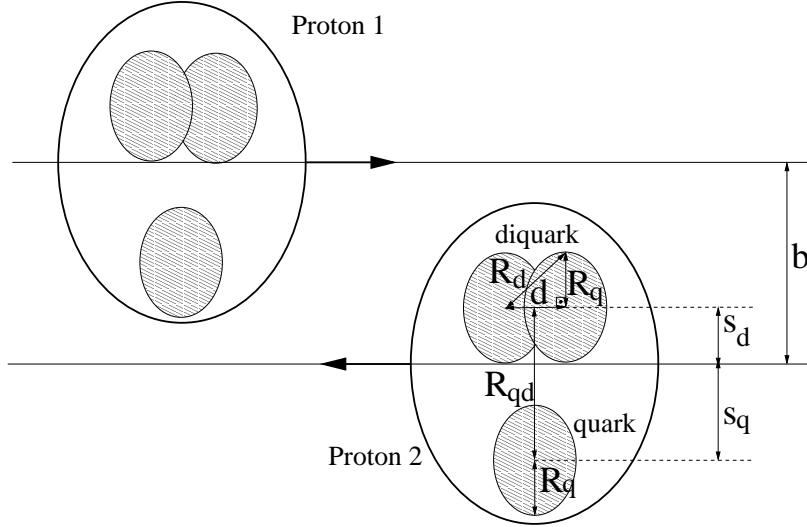


FIG. 2. The scattering situation of the two protons when the diquark is assumed to be composed of two quarks, and the proton symbolically can be written as $p=(q,(qq))$. This is just a snapshot and all the model parameters follow a Gaussian distribution.

If the internal structure of the diquark is given by eq. (15) then the σ_{qd} , σ_{dq} and σ_{dd} inelastic differential cross sections eq. (4) can be calculated from σ_{qq} using an expansion analogous to expression eq. (3). The result for σ_{qd} is the following

$$\sigma_{qd}(\vec{s}) = \frac{4A_{qq}R_q^2}{R_d^2 + R_q^2} e^{-s^2 \frac{1}{R_d^2 + R_q^2}} - \frac{A_{qq}^2 R_q^2}{R_d^2} e^{-s^2/R_q^2}, \quad (17)$$

σ_{dd} is a bit more complicated [1]. The inelastic cross section of eq. (1) for this model is again obtained using expression (12).

In their original paper, Bialas and Bzdak [1] fixed the model parameters by the total cross section, the slope parameter B , the position of the dip and the position of the first diffractive maximum after the dip. This way, they determined the best values of the model parameters essentially by the method of numerical solution of four equations containing four parameters, and found, that the resulting solution gives a good overall description of elastic scattering data at ISR energies.

In the first phase of our studies, we confirmed their results, and noted that if we want to determine the errors on the model parameters a different strategy is needed. As we were interested in finding significant dependence of the model parameters on the colliding energy, for which the estimation of the errors on the model parameters is essential, we started to improve on the original method of Bialas and Bzdak by a multiparameter fit utilizing all the available information in the data set, determining the best confidence levels and the errors on the model parameters.

In the next section, we present the final results of this multi-parameter optimization method. This manner, we improve on the earlier analysis of Bialas and Bzdak [1] with the help of the CERN Minuit package, in both cases: when the diquark acts as a single object, and also when the diquark is considered as an object composed of two quarks. We perform these analysis for all the energies where p+p elastic scattering data are available from the ISR collider, and we apply the same kind of analysis also to recent TOTEM data at $\sqrt{s} = 7$ TeV at CERN LHC energy.

Our final analysis results of p+p elastic scattering data are presented for data sets that are restricted to exactly the same kinematic domain at all the five considered energies. We also study, in addition to the differential cross-section of elastic scattering, the effect of including the measured total p+p scattering cross-section data to the fitting procedure, at all the four ISR and also at $\sqrt{s} = 7$ TeV LHC energies.

Finally, we summarize and conclude.

III. FINAL MINUIT FIT RESULTS TO P+P ELASTIC SCATTERING DATA AT ISR AND LHC ENERGIES

A. Model $p = (q, d)$: The diquark is assumed to scatter as a single entity

In this section the MINUIT fit results are presented for the ISR [25, 26] and TOTEM [7] proton-proton elastic scattering data considering the scenario when the diquark is assumed to act as a single entity in this scattering process. Our preliminary analysis of these data, that did not yet study the correlations between model parameters and also did not evaluate what happens if some of the model parameters are fixed, was presented in a recent conference contribution [5].

Our final results are illustrated on Figs. 3-7. The confidence levels, and model parameters together with their errors are presented in Table I. The calculated total elastic cross sections, including their uncertainty, were evaluated from the MINUIT fits to the differential cross section data, restricted to the same intermediate t elastic scattering. At the end of this section we also study and discuss, what happens when the measured total elastic cross sections are also added, as an additional data point, to the optimization procedure.

The ratios of the inelastic cross sections were fixed with eq. (9), in order to decrease the number of free fit parameters, therefore these ratios will be provided only for the case, when the diquark is assumed to be a composite object.

Some additional remarks are due before our final results are presented. The Bialas - Bzdak model shows a singular behaviour at the diffractive minimum or dip position, which is due to the lack of a real part in its amplitude. In a Minuit fit, such an unphysical fit region may completely dominate the fit results. In order to avoid such an artefact and to obtain a meaningful fit result, we have excluded 3 data points from the optimization procedure, that were closest to this dip region. These points are shown in red (color online) or on the plots. We have checked that leaving out 5 or 7 points did not change the results.

Another important remark is that the TOTEM data covers the $|t|$ range from 0.36 GeV up to 2.5 GeV and this range is applied in our minimization procedure to allow a comparison between the ISR and TOTEM results. Note that Bialas and Bzdak adjusted their model in a different way: they demanded, that four important features of the data are described correctly, namely (i) the total inelastic cross-section and (ii) the slope of the differential cross-section as extrapolated to $t = 0$, and (iii) the position of the first diffractive minimum and finally (iv) the height of the diffractive maximum after the diffractive minimum [1]. A different strategy is followed here, since we have fitted the theoretical curve directly to the experimental data points using the CERN MINUIT package by minimizing χ^2 . However, we selected the same reasonable t -range for all data sets, and we left out data points around the diffractive minimum, where this model clearly breaks down. These data points are clearly indicated with filled (color online red) circles in the subsequent Figures, where the fit results are shown and can be compared to data directly.

In a preliminary analysis, reported in ref. [5], all model parameters were optimized, including also the values of λ and A_{qq} . Those preliminary results are compatible with the final fits presented here, however, in those results large correlations remained among the fit parameters, and their errors were correspondingly large. The optimization process indicated that the parameters λ and A_{qq} were in the range of their nominal value and fixing them resulted in considerable reduction of correlations among the other model parameters. Hence in the final fits presented here we utilized fixed values of $\lambda = 0.5$ and $A_{qq} = 1.0$.

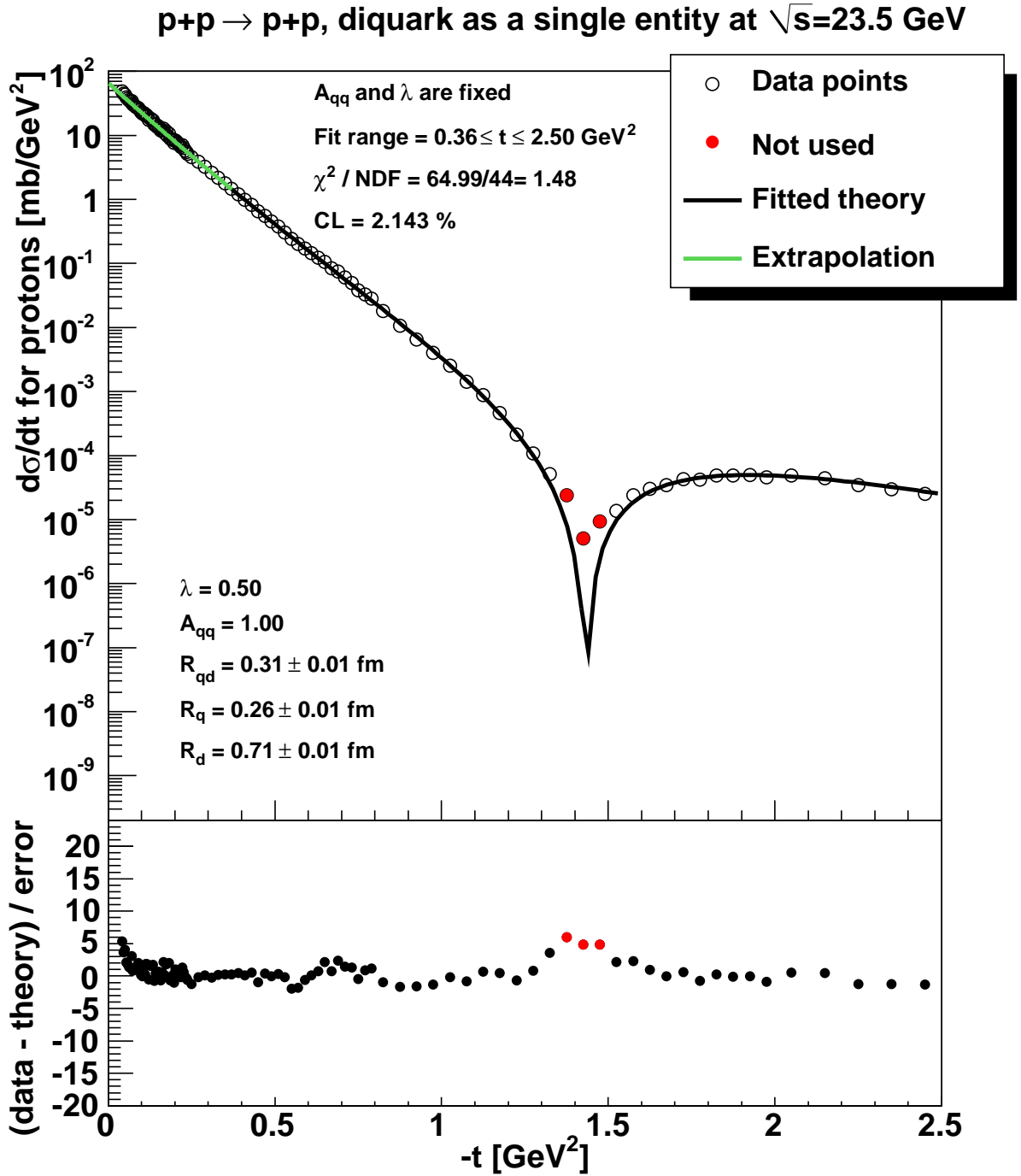


FIG. 3. (Color online.) Results of MINUIT fits at ISR energies when the diquark is assumed to scatter as a single entity. Top panel shows the data points and the result of the best fit, while the lower panel shows the relative deviation of the model from data in units of measured error bars. As the model is singular around the dip, 3 data points that are located closest to this diffractive minimum and are indicated with filled (red) circles in this Figure, were left out from the fit. The optimization was restricted to the 0.36 - 2.5 GeV $|t|$ range, so that a fair comparison could subsequently be made with most recent TOTEM results as given in ref. [7]. The best fit is indicated with a solid (black) line in this range and its extrapolation to low values of t are also shown. The confidence level, after fixing the values of λ and A_{qq} , is still higher than 0.1%, which indicates that this fit quality is statistically acceptable.

$p+p \rightarrow p+p$, diquark as a single entity at $\sqrt{s}=30.7$ GeV

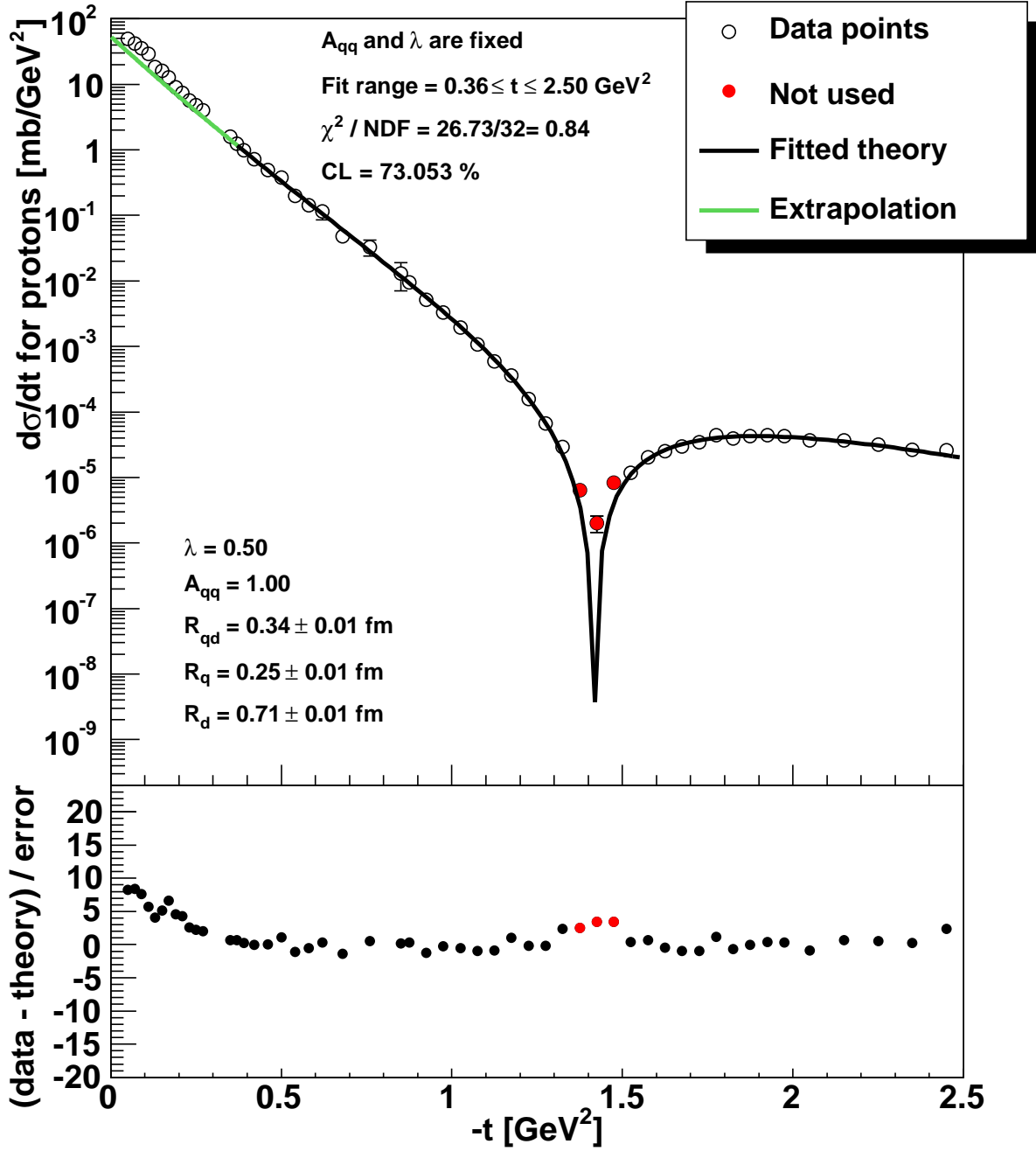


FIG. 4. (Color online.) Same as Fig. 3, but for the energy $\sqrt{s} = 30.7$ GeV.

$p+p \rightarrow p+p$, diquark as a single entity at $\sqrt{s}=52.8$ GeV

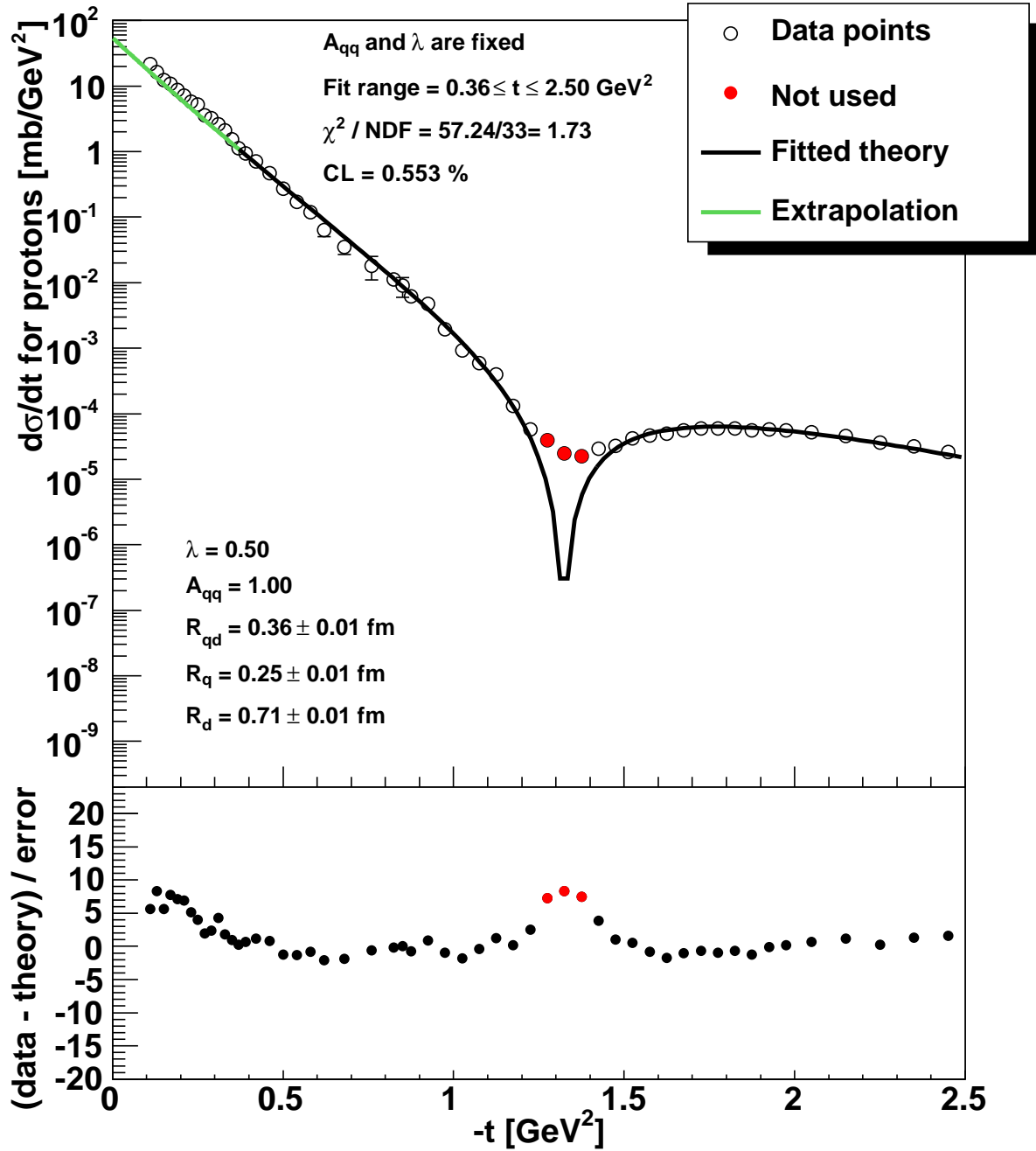


FIG. 5. (Color online.) Same as Fig. 3, but for the energy $\sqrt{s} = 52.8$ GeV.

$p+p \rightarrow p+p$, diquark as a single entity at $\sqrt{s}=62.5$ GeV

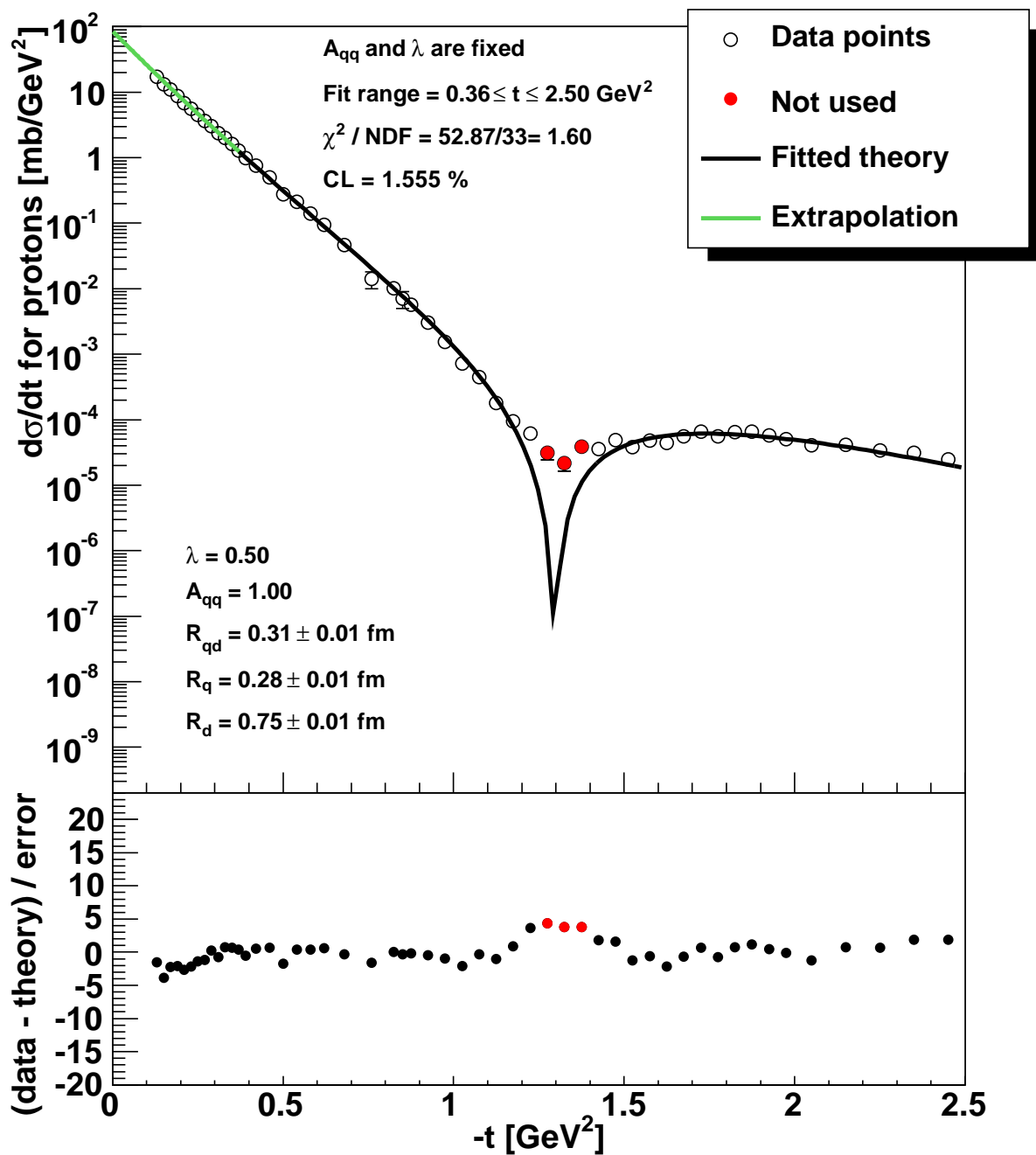


FIG. 6. (Color online.) Same as Fig. 3, but for the energy $\sqrt{s} = 62.5$ GeV.

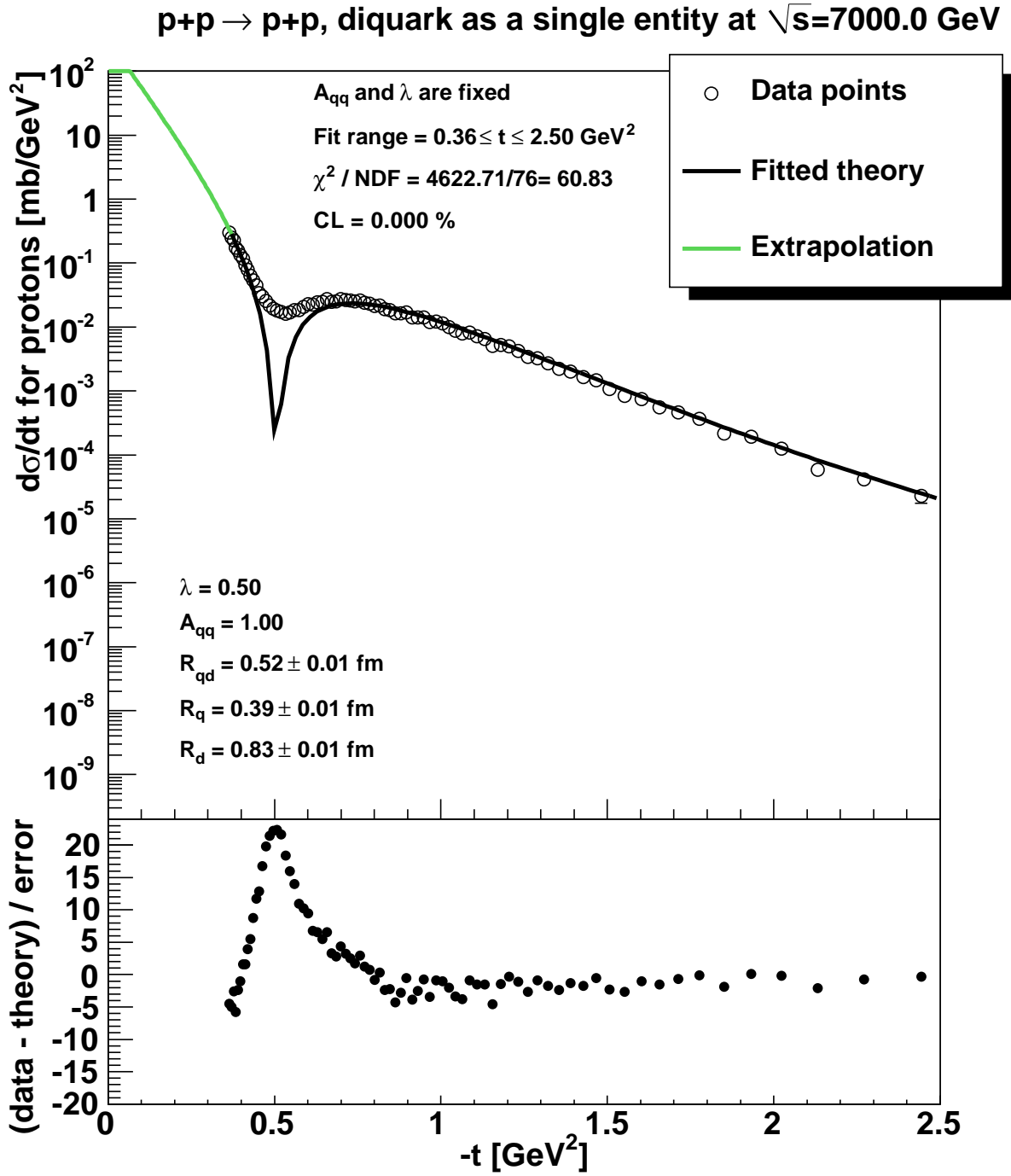


FIG. 7. (Color online.) The result of the fit at LHC at 7 TeV when the diquark is assumed to scatter as a single entity, $p = (q, d)$. Note that CL is below 0.1%, so the quality of this fit is not acceptable. The bottom panel indicates, that the shape of the diffractive cross-section around the first diffractive minimum is not reproduced correctly by this model at LHC energies, and – as can also be seen on this Figure – this shortcoming cannot be fixed by leaving out a few data points around this dip from the optimization procedure.

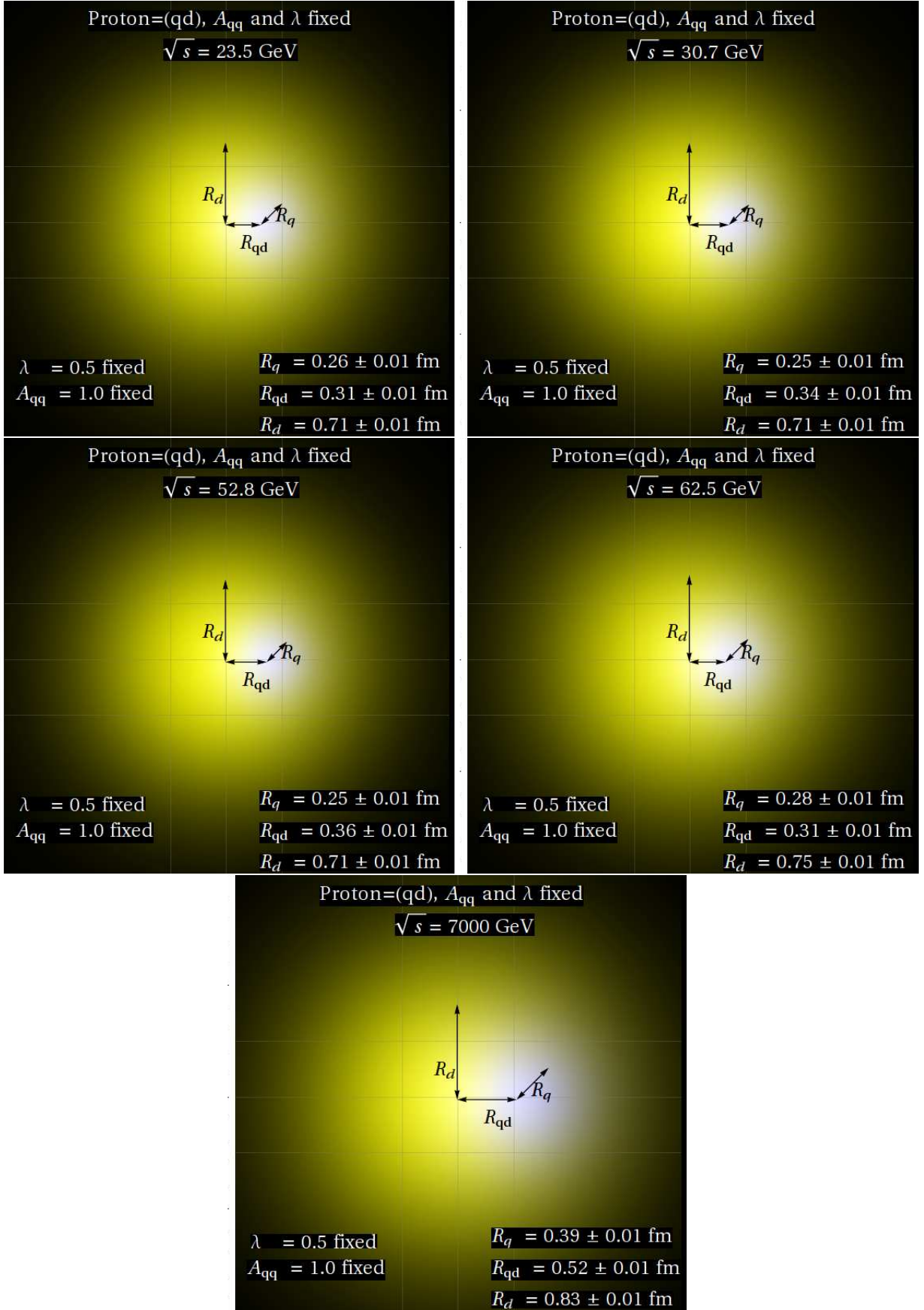


FIG. 8. (Color online.) Visualisation of the obtained R_{qd} , R_q , R_d parameters for the case when the proton is assumed to scatter as a quark-diquark composit, $p = (q, d)$ and $A_{qq} = 1$, $\lambda = 0.5$ fixed. The main observation is that the proton seems to be much larger at LHC energies than at ISR regime. This is mainly due to an increase in the R_{qd} parameter, that characterizes the separation of the quark and the diquark.

\sqrt{s} [GeV]	23.5	30.7	52.8	62.5	7000
λ	0.5	0.5	0.5	0.5	0.5
A_{qq}	1.00	1.00	1.00	1.00	1.00
R_{qd} [fm]	0.31 ± 0.01	0.34 ± 0.01	0.36 ± 0.01	0.31 ± 0.01	0.52 ± 0.01
R_q [fm]	0.26 ± 0.01	0.25 ± 0.01	0.25 ± 0.01	0.28 ± 0.01	0.39 ± 0.01
R_d [fm]	0.71 ± 0.01	0.71 ± 0.01	0.71 ± 0.01	0.75 ± 0.01	0.83 ± 0.01
χ^2/NDF	65.0/44	26.7/32	57.2/33	52.9/33	4622.7/76
CL [%]	2.14	73.05	0.55	1.56	0.0
$\sigma_{elastic}$ [mb]	6.2 ± 0.1	5.1 ± 0.3	5.0 ± 0.3	7.3 ± 0.3	17.9 ± 0.2

TABLE I. The overall fit quality and resulting parameters of the fit at ISR energies including the LHC result at 7 TeV. The diquark is assumed to be a single entity.

B. Model $p = (q, (q, q))$: diquark scatters as composite object

In this subsection, similar MINUIT fit results are presented as in the previous subsection, the main modification is a change in the model assumption: now we assume that the diquark scatters as a composite object that contains two quarks. We present the final fit results to proton-proton elastic scattering data both at ISR [25, 26] and at LHC energies [7]. The results are illustrated on Fig. 9-13. The confidence levels, and model parameters with their errors are summarized in Table II.

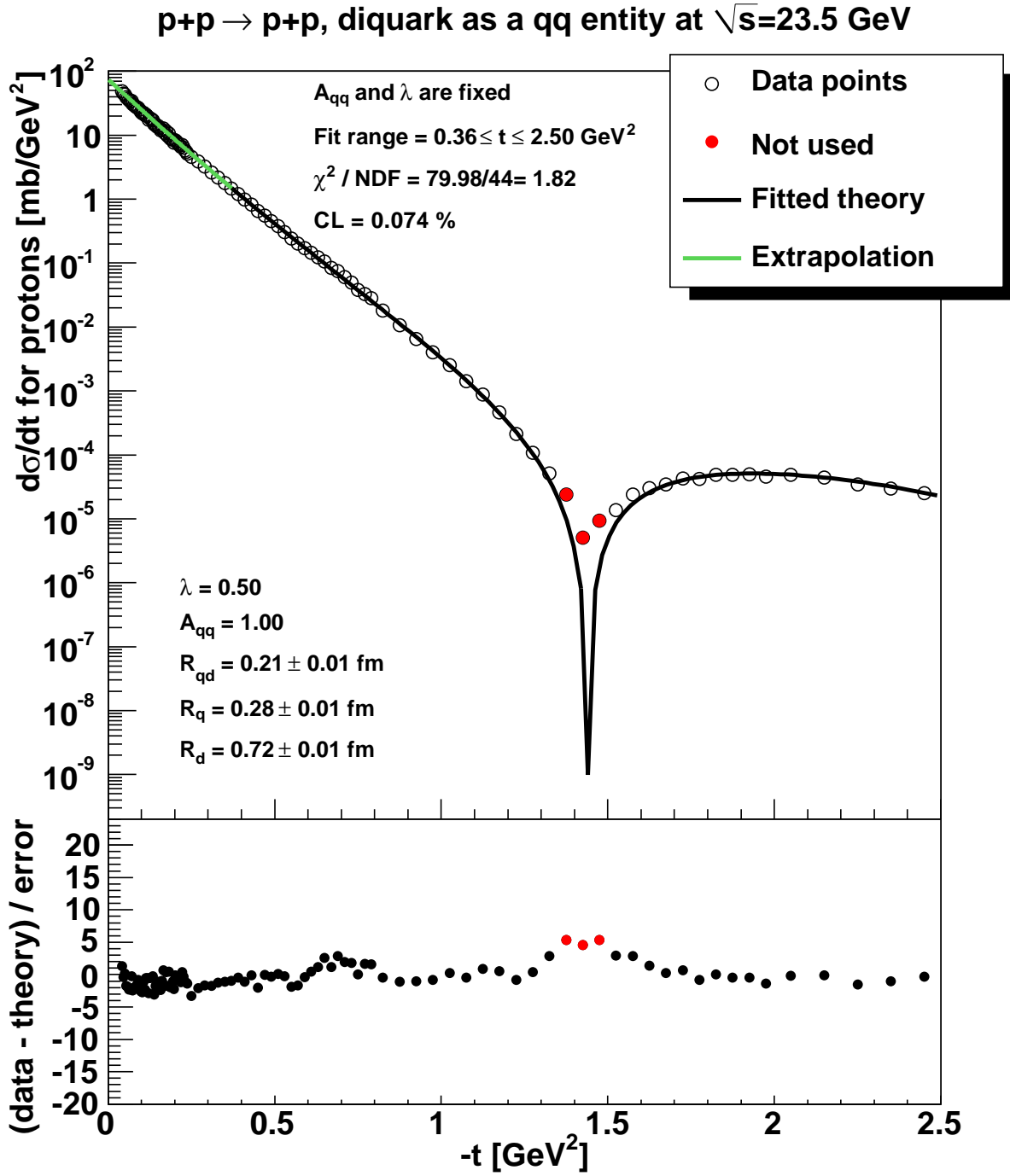


FIG. 9. (Color online.) Same as Fig. 3, but the diquark is assumed to have a composite (q, q) substructure.

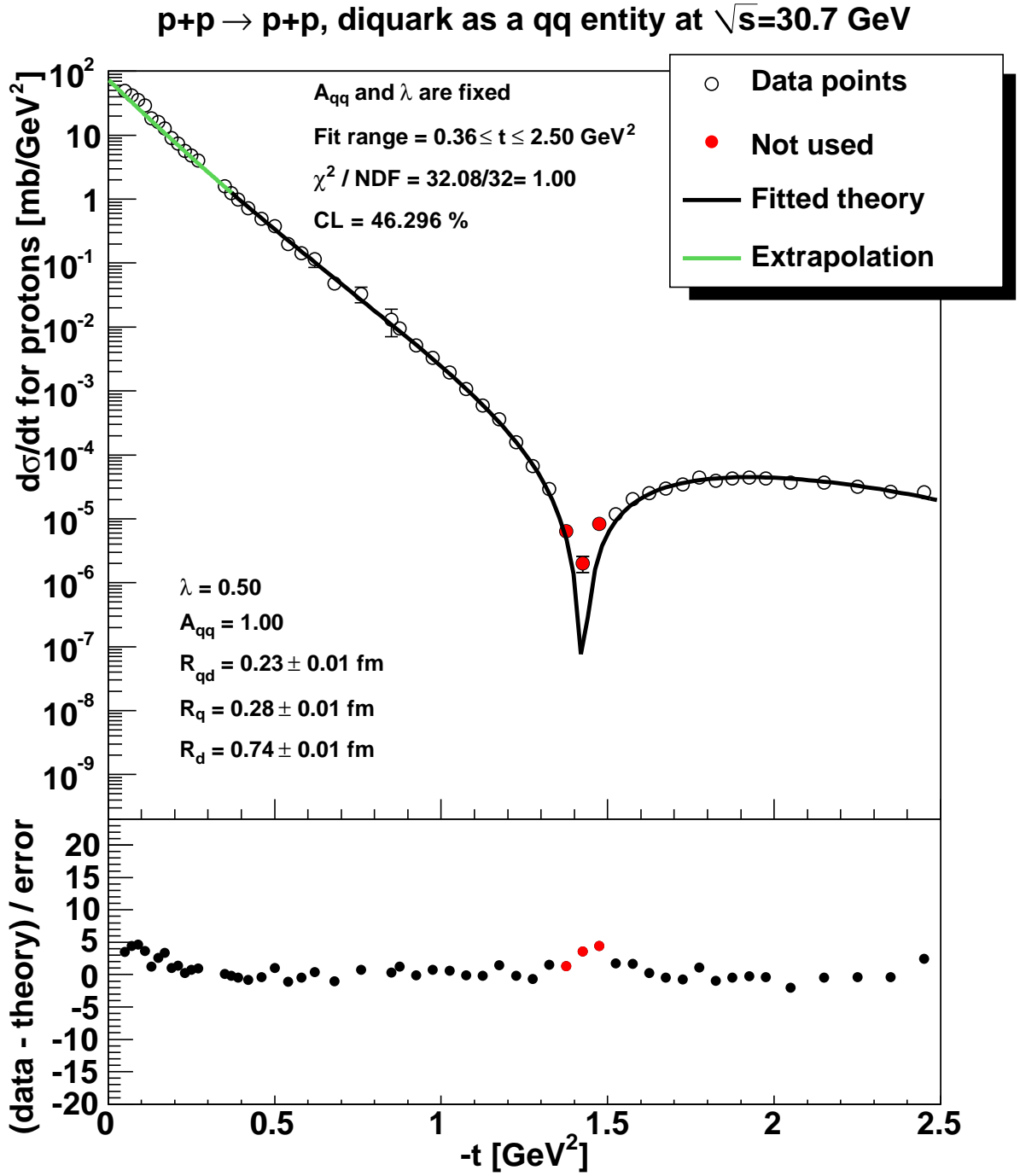


FIG. 10. (Color online.) Same as Fig 9, but for $\sqrt{s} = 30.7$ GeV.

$p+p \rightarrow p+p$, diquark as a qq entity at $\sqrt{s}=52.8$ GeV

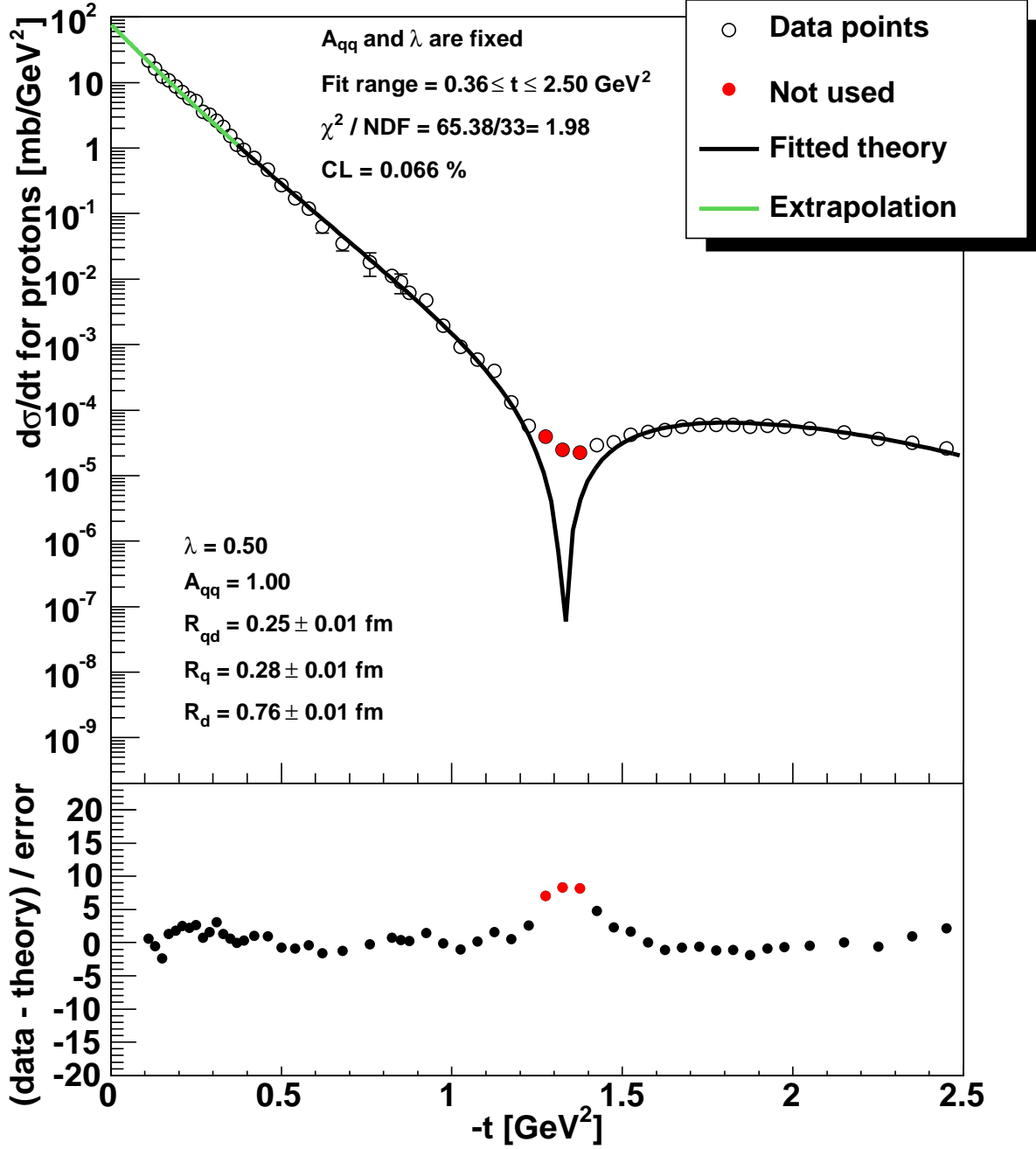


FIG. 11. (Color online.) Same as Fig 9, but for $\sqrt{s} = 52.8$ GeV.

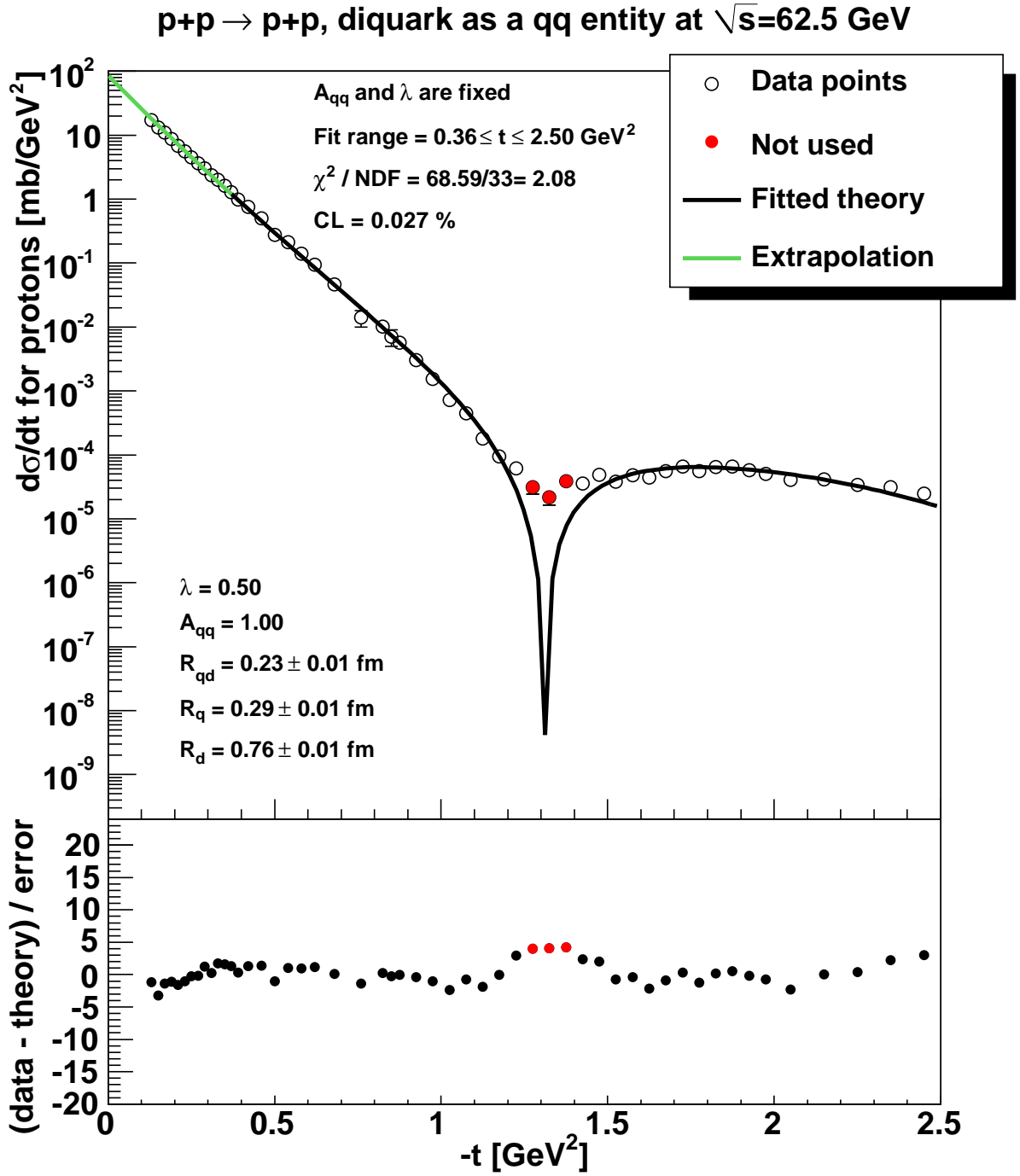


FIG. 12. (Color online.) Same as Fig 9, but for $\sqrt{s} = 62.5$ GeV.

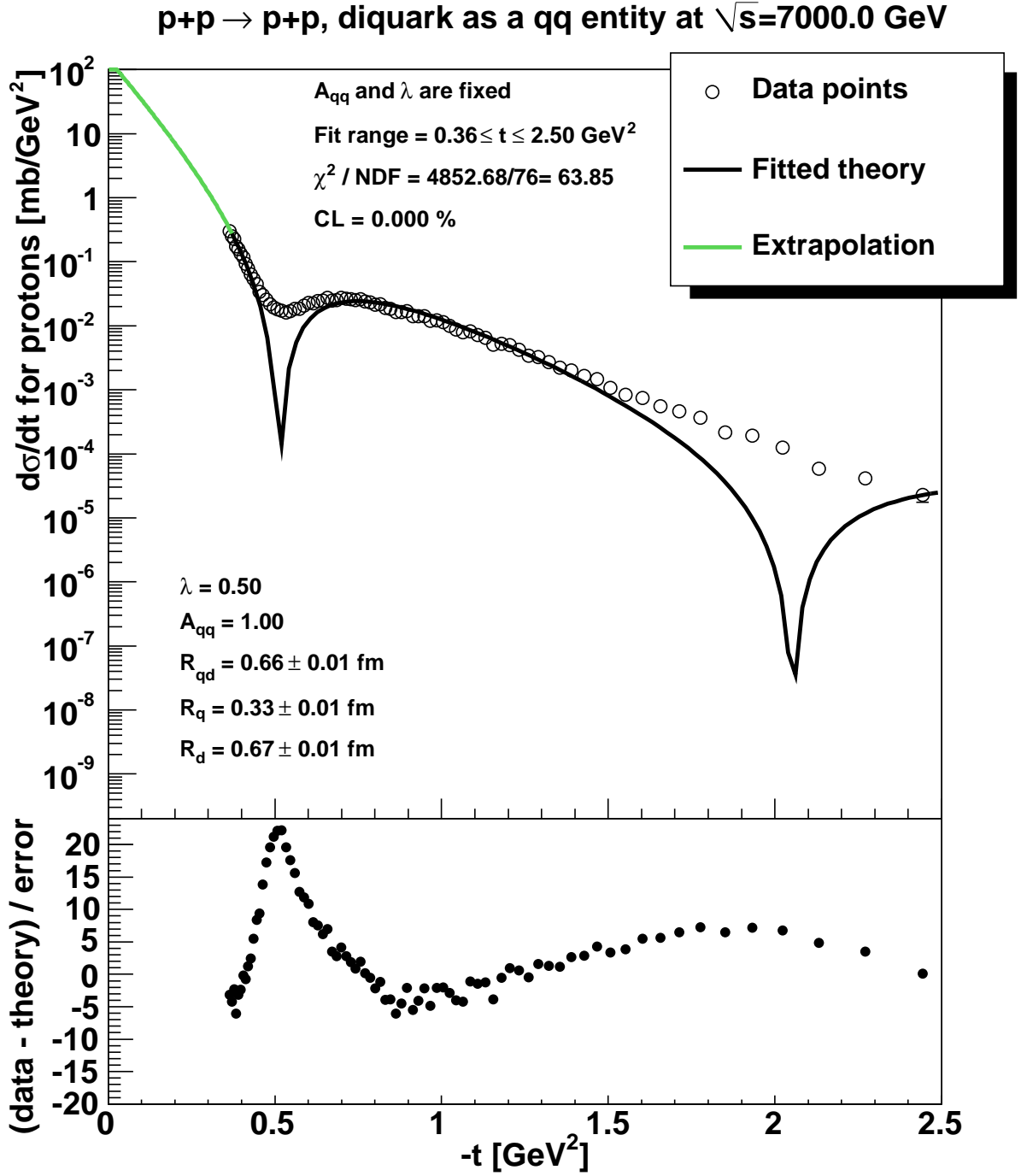


FIG. 13. (Color online.) Same as Fig 9, but for $\sqrt{s} = 7$ TeV. Note that this fit is not acceptable, since its CL is below 0.1%.

C. Total cross sections in the $p = (q, (q, q))$ model: the diquark is considered to be a composite object.

The total inelastic cross sections for the quark-quark, quark-diquark and diquark-diquark subcollisions were analyzed on the basis of formula (4). The detailed results are collected in Table III, while the average of these ratios for the described ISR energies are

\sqrt{s} [GeV]	23.5	30.6	52.8	62.5	7000
λ	0.50	0.50	0.50	0.50	0.50
A_{qq}	1.00	1.00	1.00	1.00	1.00
R_{qd} [fm]	0.21 ± 0.01	0.23 ± 0.01	0.25 ± 0.01	0.23 ± 0.01	0.66 ± 0.01
R_q [fm]	0.28 ± 0.01	0.28 ± 0.01	0.28 ± 0.01	0.29 ± 0.01	0.33 ± 0.01
R_d [fm]	0.72 ± 0.01	0.74 ± 0.01	0.76 ± 0.01	0.76 ± 0.01	0.67 ± 0.01
χ^2/NDF	80.0/44	32.1/32	65.4/33	68.6/33	4852.7/76
CL [%]	0.07	46.30	0.07	0.03	0.0
$\sigma_{elastic}$ [mb]	6.9 ± 0.1	6.6 ± 0.1	6.6 ± 0.1	7.2 ± 0.1	9.8 ± 0.1

TABLE II. The overall fit quality and resulting parameters of the fit at the ISR energies including the LHC result at 7 TeV. The diquark is assumed to be a $d = (q, q)$ composit entity.

\sqrt{s} [GeV]	23.5	30.6	52.9	62.5	7000
σ_{qd}/σ_{qq}	1.92 ± 0.01	1.93 ± 0.01	1.93 ± 0.01	1.93 ± 0.01	1.88 ± 0.01
σ_{dd}/σ_{qq}	3.64 ± 0.02	3.66 ± 0.01	3.67 ± 0.01	3.65 ± 0.01	3.43 ± 0.02

TABLE III. The ratios of the total inelastic cross sections for the quark-quark, quark-diquark and diquark-diquark processes for the ISR and LHC energies using the composite diquark hypothesis.

$$\sigma_{qq} : \sigma_{qd} : \sigma_{dd} = 1 : (1.93 \pm 0.03) : (3.65 \pm 0.1), \quad (18)$$

which is close to the ideal 1 : 2 : 4 ratio, confirming the assumption of having two quarks inside the diquark, amended with some shadowing which is 4% and 9% respectively. At 7 TeV the ratios are different from (18)

$$1 : (1.88 \pm 0.01) : (3.43 \pm 0.02), \quad (19)$$

which shows that shadowing is stronger, 6% and 14% percent respectively, and a significant decrease compared to the ideal ratio can be observed.

The total elastic scattering cross sections were also determined, as given in Table II. In a preliminary conference proceedings [5], we have noted that that the errors on the total elastic cross sections might be decreased by fixing the A_{qq} and λ parameters to their nominal values of 1 and 0.5, respectively. Our final results presented here confirm this conjecture.

\sqrt{s} [GeV]	23.5	30.6	52.9	62.5	7000
data [mb]	38.94 ± 0.17	40.14 ± 0.17	42.67 ± 0.19	43.32 ± 0.23	98.3 ± 0.2
p=(q,d)					
σ_{total} [mb]	38.5 ± 0.2	40.0 ± 0.2	42.5 ± 0.2	43.2 ± 0.3	79.0 ± 1.1
χ^2/NDF	107.2/45	62.2/33	110.7/34	56.1/34	4667.67/77
CL [%]	0.00	0.16	0.00	1.00	0.00
p=(q,(q,q))					
σ_{total} [mb]	38.6 ± 0.1	39.7 ± 0.2	41.6 ± 0.2	42.6 ± 0.2	74.2 ± 1.3
χ^2/NDF	86.8/45	60.2/33	154.2/34	95.3/34	5059.57/77
CL [%]	0.02	0.26	0.00	0.00	0.00

TABLE IV. Measured and fitted values of the total cross sections, when the measured values of the total cross sections are included into the earlier fitting procedure, as another, additional data point.

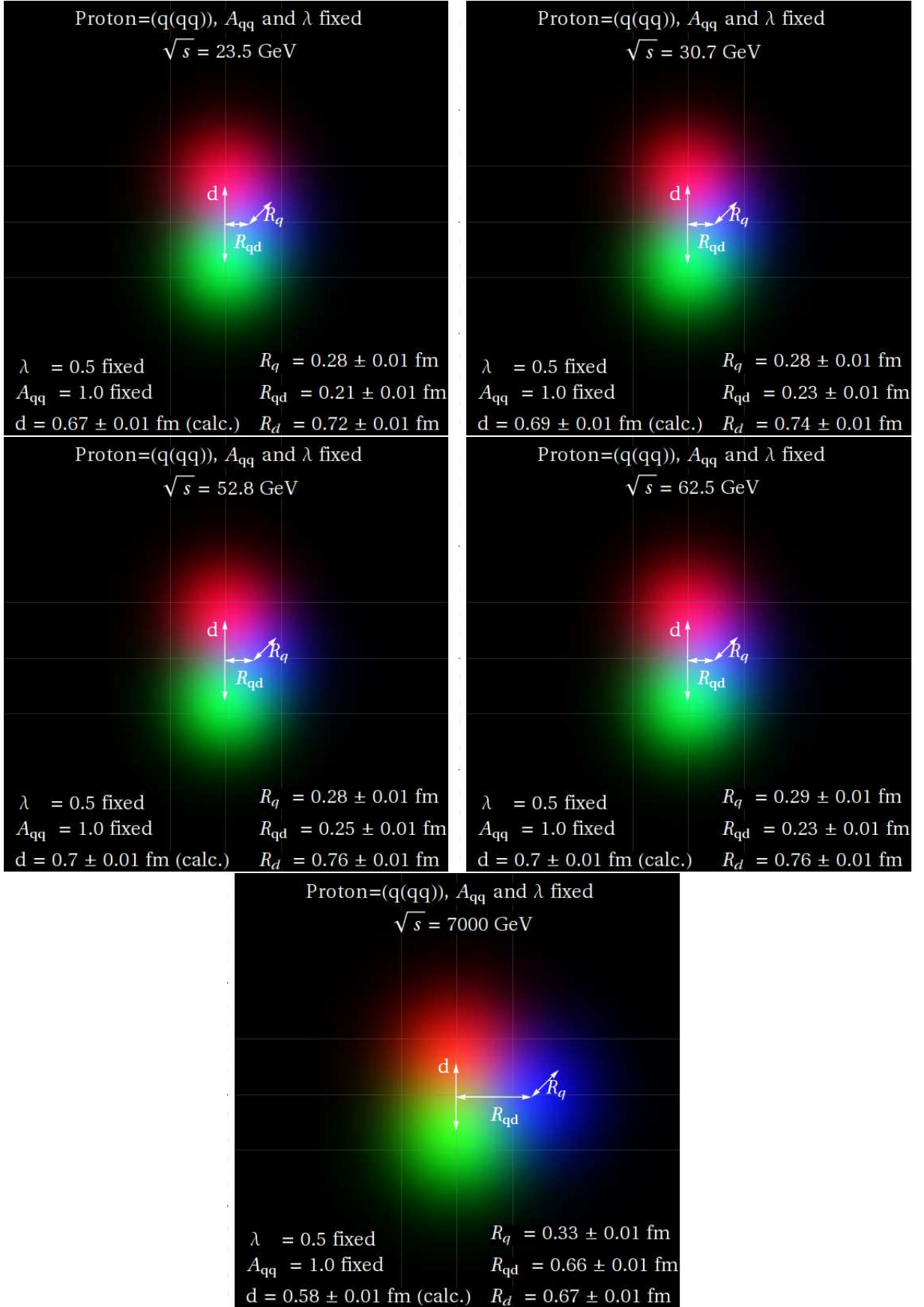


FIG. 14. (Color online.) Visualisation of the obtained R_{qd} , R_q , R_d parameters when the diquark is assumed to be a qq entity. The proton seems to be much larger at LHC energies than in the ISR regime. This is mainly due to an increase in the R_{qd} parameter, that characterizes the separation of the quark and the diquark, which is further decomposed as (q,q) state in this class of models.

D. Model comparison

The \sqrt{s} dependence of the parameters is summarized here. The confidence levels as a function of the center of mass energy for both of the models are given on Fig. 15. We left out the confidence level for TOTEM which is zero, all the other values are higher than or close to 0.1%.

The center of mass energy dependence of the quark-diquark distance is presented on Fig. 16. The effective quark radius can be seen on Fig. 17 and the obtained diquark radius is on Fig. 18.

As can be seen on these figures, the fit quality is similar and the best fit parameters are rather different for both models at each colliding energies and the picture of the protons as realized by Figs. 8 and 14 are rather different. We started to wonder how it is possible, that the apparently rather different $p=(q,d)$ and $p=(q,(q,q))$ models give so similar fit results, not only quantitatively but qualitatively too? Although the mathematical equations that describe the $d\sigma/dt$ from the two models are rather complex and formally different from one another, we investigated some simple relationships among the model parameters.

Numerically, we found one combination of the model parameters, an effective radius that is obtained from the quadratic sum of R_q , R_d and R_{qd} , that seems to be the same in both models and which is related in a simple way to the measured total cross-section.

$$R_{\text{eff}} = \sqrt{R_q^2 + R_d^2 + R_{qd}^2}, \quad (20)$$

$$\sigma_{\text{total}} = 2\pi R_{\text{eff}}^2. \quad (21)$$

The \sqrt{s} dependence of the effective radius R_{eff} is shown on Figure 19, and the relationship between the effective radius and the measured total cross section is presented on Figure 20.

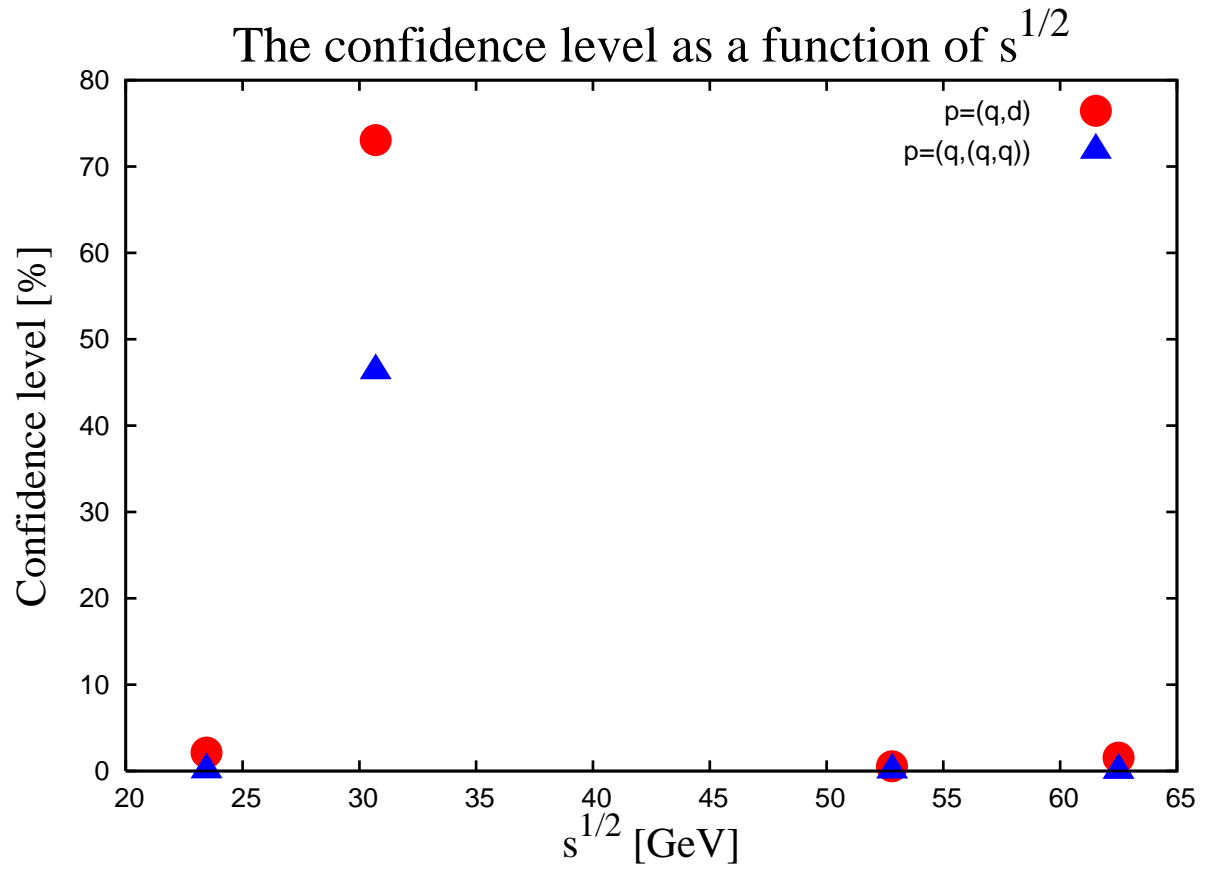


FIG. 15. (Color online.) The confidence level as a function of \sqrt{s} . The value of CL at 7 TeV is practically zero and it is not shown.

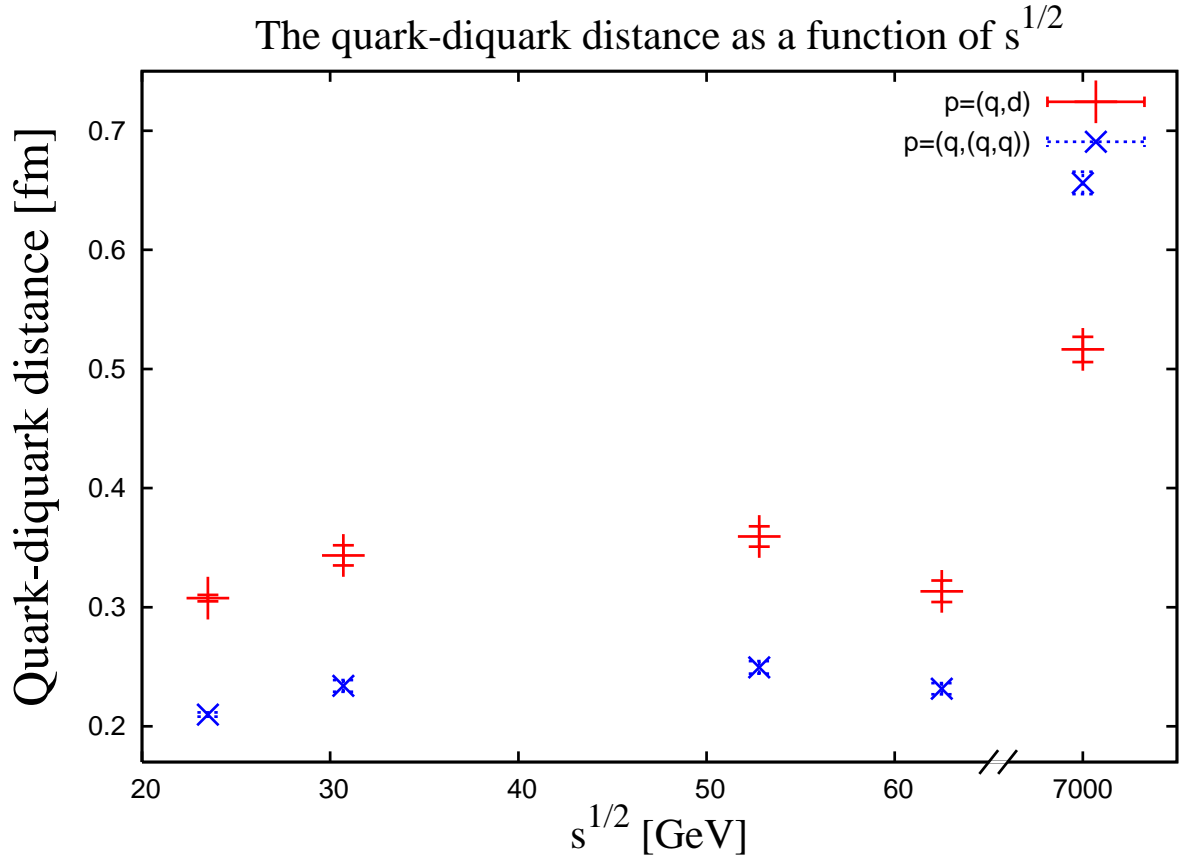


FIG. 16. (Color online.) Parameter R_{qd} , representing the separation of the quark and the diquark, as a function of \sqrt{s} .

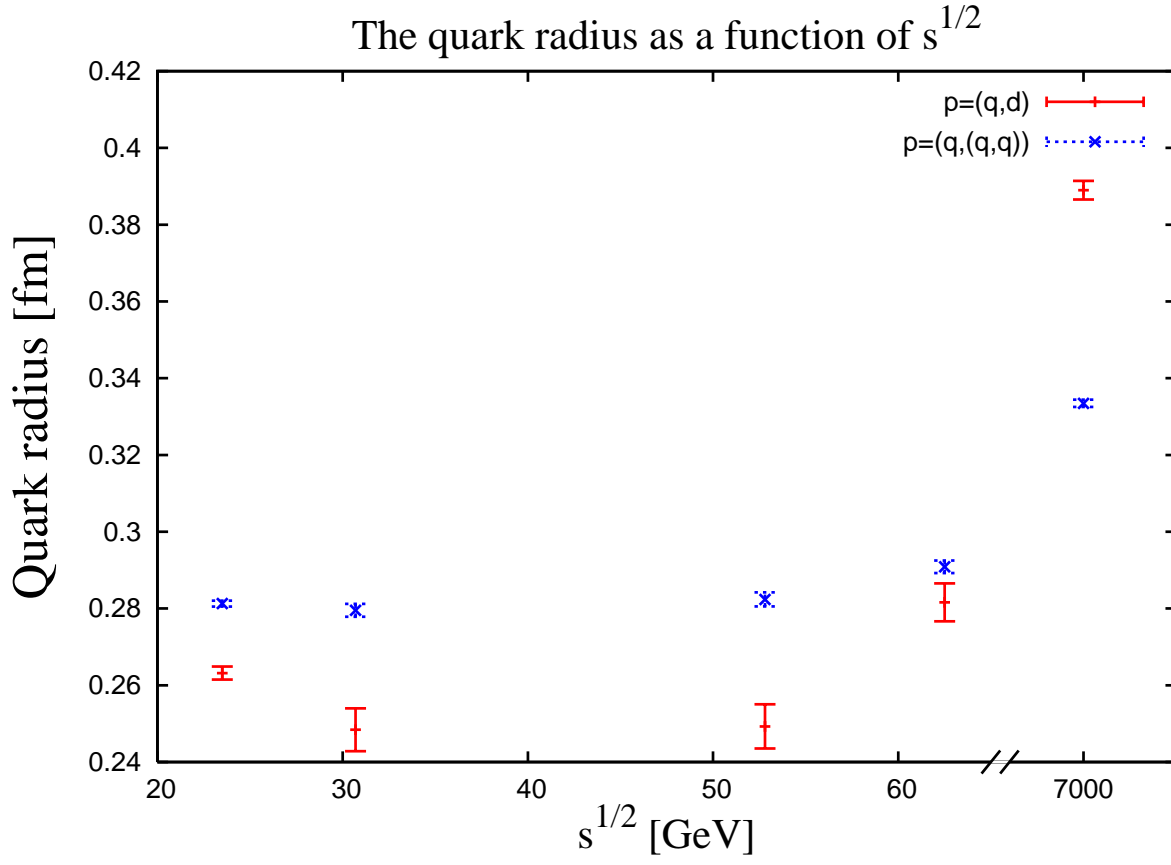


FIG. 17. (Color online.) Parameter R_q (quark size) as a function of \sqrt{s} .

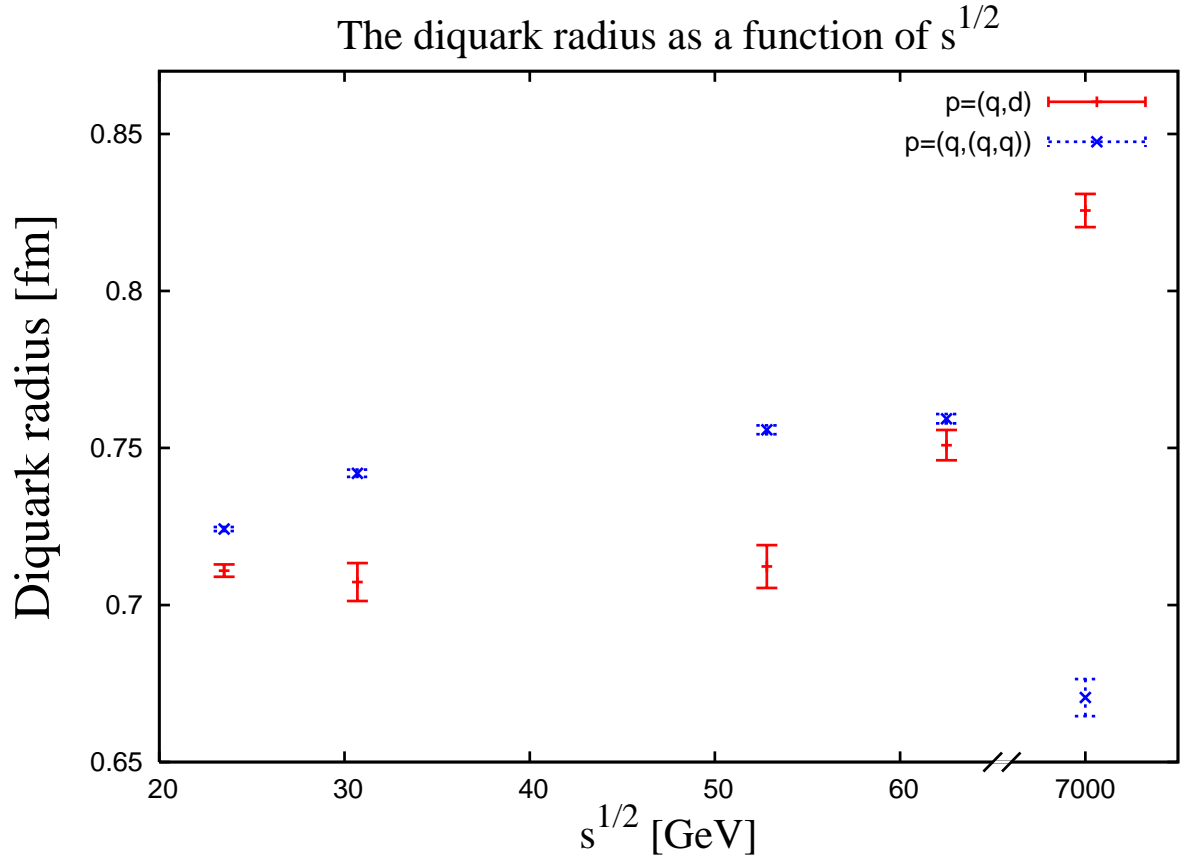


FIG. 18. (Color online.) Parameter R_d , the diquark size, as a function of \sqrt{s} .

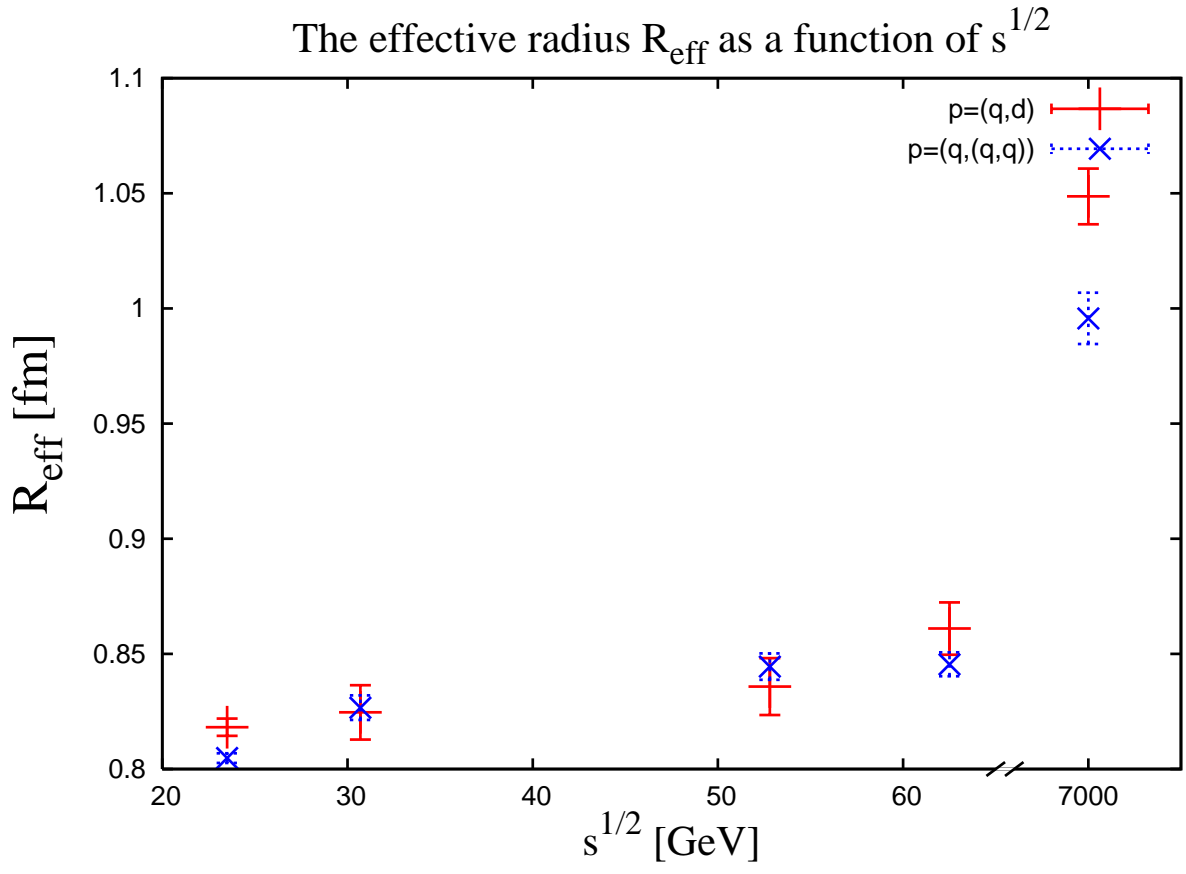


FIG. 19. (Color online.) The model independent R_{eff} radius parameter as a function of \sqrt{s} .

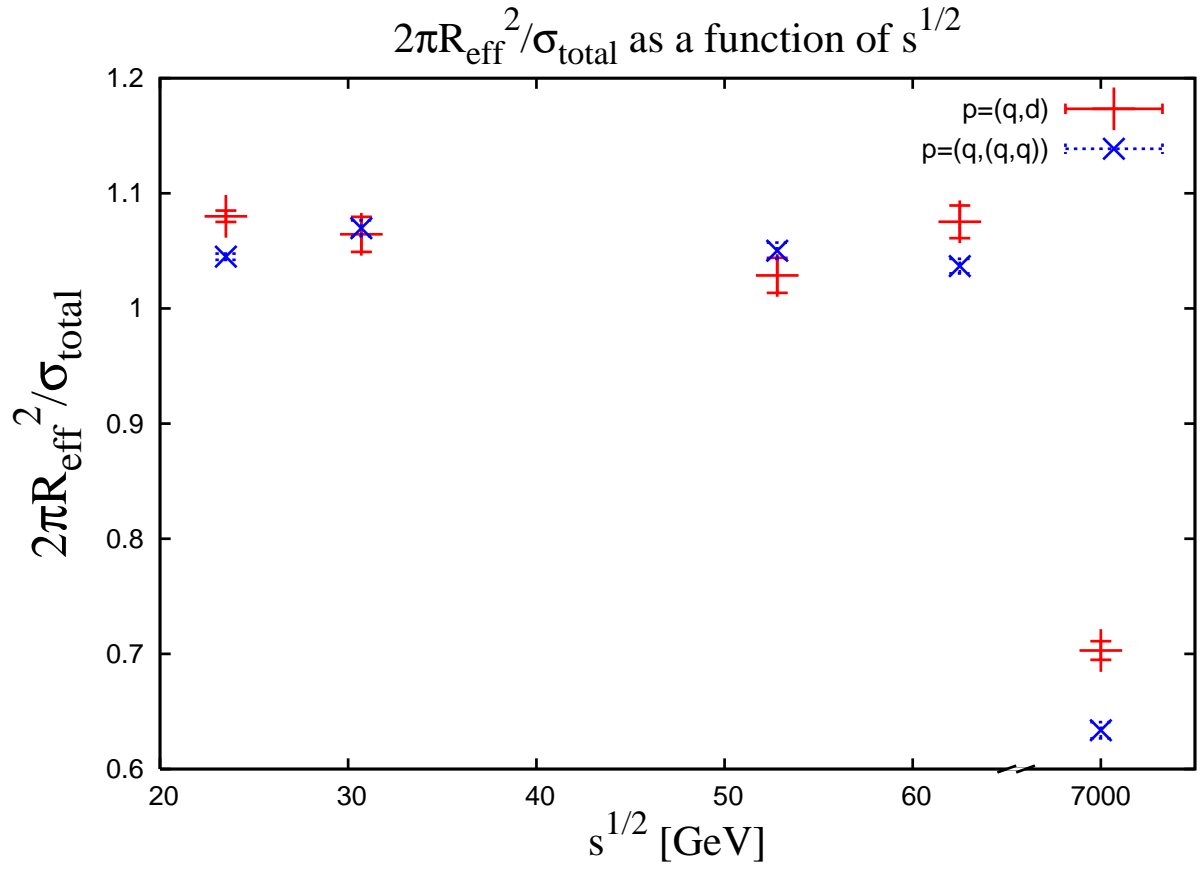


FIG. 20. (Color online.) The effective R_{eff} radius divided by the measured total cross section as a function of \sqrt{s} . The result indicates a simple relationship between these parameters, namely, both for the case when a proton is modelled as $p = (q,d)$ and for the case when $p = (q, (q,q))$, the quadratic sum of the characteristic radii is the same model independent quantity.

IV. CONCLUSION AND OUTLOOK

A systematic study of fit quality as well as the fit parameters under similar circumstances have been performed for the Bialas - Bzdak model [1] in a wide energy range from ISR to LHC energies using the same kinematic interval and the same method at each energy. The model gives a good description of the ISR data, which means that the CL is acceptable on the ISR energies if 3 data points at first diffractive minimum were left out from the fit. These studies confirm earlier results [1] concerning the increase of the total proton-proton cross section (“size” of the proton) with increased colliding energies.

An important shortcoming of the quark-diquark model of protons is that it ignores the real part of the elastic scattering amplitude. This leads to a singular behaviour at the diffractive minimum, which is apparently a more and more serious model limitation with increasing the energy of p+p collisions. Due to this reason, the considered model fails to describe in detail the structure of the first diffractive minimum at the LHC energies of 7 TeV.

We found a combination of the model parameters, an effective radius that is obtained as the quadratic sum of quark, diquark radii and the separation between the quark and the center of mass of the diquark, that seems to be the same in both models and which is related in a simple, intuitive way to the measured total cross-section, as given by eqs. (20) and (21). As indicated on Figure 20, the precision of this ”rule of thumb” formula is about 10 % which is quite amazing for us given that it is an extremely simple formula as compared to the full, exact and analytic expressions that are also obtained from both models.

The evaluated ratios of the quark-quark, quark-diquark and diquark-diquark total inelastic cross-sections were found to deviate more and more from the ideal 1 : 2 : 4 ratio with increasing energies. In the ISR energy range the deviations from this ideal value were less than a 5σ effect, indicating lack of significant shadowing effects. However at the current LHC energy of $\sqrt{s} = 7$ TeV, a significant decrease – as indicated by eq. (19) – compared to these ideal ratios were found, which possibly may indicate an increased role of shadowing at CERN LHC energies.

Finally let us note that the TOTEM Collaboration extended recently the measurement of the differential elastic p+p scattering cross-sections to low values of $|t|$ in ref. [27], allowing one to extrapolate to the optical point at $t = 0$ and to determine the total elastic and the total scattering cross-sections of p+p collisions at $\sqrt{s} = 7$ TeV for the first time, but these data were yet not utilized in our analysis.

V. ACKNOWLEDGEMENTS

T. Cs. would like to thank prof. R. J. Glauber for valuable discussions at the initial phase of this project, and for his kind hospitality at Harvard University and to I. Dremin for inspiring discussions. F. N. would like to thank A. Ster and M. Csanád for their valuable help with the CERN MINUIT multi-parameter optimization. The authors would like to thank R. Lohner for a careful reading of the draft of this manuscript. This research was partially supported by the Hungarian American Enterprise Scholarship Fund (HAESF) and by the Hungarian OTKA grant NK 101438.

-
- [1] A. Bialas and A. Bzdak, *Acta Phys. Polon. B* **38** (2007) 159 [hep-ph/0612038].
- [2] A. Bzdak, *Acta Phys. Polon. B* **38** (2007) 2665 [hep-ph/0701028].
- [3] A. Bialas and A. Bzdak, *Phys. Lett. B* **649** (2007) 263 [nucl-th/0611021].
- [4] A. Bialas and A. Bzdak, *Phys. Rev. C* **77** (2008) 034908 [arXiv:0707.3720 [hep-ph]].
- [5] F. Nemes and T. Csörgő, arXiv:1202.2438 [hep-ph].
- [6] F. James and M. Roos, *Comput. Phys. Commun.* **10** (1975) 343.
- [7] G. Antchev *et al.* [TOTEM Collaboration], *Europhys. Lett.* **95**, 41001 (2011) [arXiv:1110.1385 [hep-ex]].
- [8] D. A. Fagundes, E. G. S. Luna, M. J. Menon and A. A. Natale, arXiv:1108.1206 [hep-ph].
- [9] A. D. Martin, M. G. Ryskin and V. A. Khoze, arXiv:1110.1973 [hep-ph].
- [10] A. Donnachie and P. V. Landshoff, arXiv:1112.2485 [hep-ph].
- [11] D. A. Fagundes, E. G. S. Luna, M. J. Menon and A. A. Natale, arXiv:1112.4680 [hep-ph].
- [12] M. G. Ryskin, A. D. Martin and V. A. Khoze, arXiv:1201.6298 [hep-ph].
- [13] M. M. Block and F. Halzen, arXiv:1201.0960 [hep-ph].
- [14] T. Wibig, arXiv:1111.0441 [hep-ph].
- [15] For a recent summary of the discovery of the exotic hadrons XYZ see the KEK press release at <http://www.kek.jp/intra-e/press/2012/011014/> .
- [16] M. Kreps [Belle and Babar Collaborations], *PoS BEAUTY* **2009** (2009) 038 [arXiv:0912.0111 [hep-ex]].
- [17] A. Adare *et al.* [PHENIX Collaboration], *Phys. Rev. Lett.* **103** (2009) 012003 [arXiv:0810.0694 [hep-ex]].
- [18] A. Bialas, K. Fialkowski, W. Slominski and M. Zielinski, *Acta Phys. Polon. B* **8**, 855 (1977)
- [19] R. J. Glauber, *Phys. Rev.* **100** (1955) 242.
- [20] R. J. Glauber, *Nucl. Phys. A* **774** (2006) 3 [nucl-th/0604021].
- [21] R. J. Glauber, *Lectures in Theoretical Physics*, ed. W. E. Brittin and L. G. Dunham (Interscience Publishers, New York, 1959), vol. 1, p. 315.
- [22] W. Czyz and L. C. Maximon, *Annals Phys.* **52** (1969) 59.
- [23] I. M. Dremin and V. A. Nechitailo, arXiv:1202.2016 [hep-ph].
- [24] I. M. Dremin, arXiv:1204.1914 [hep-ph].
- [25] E. Nagy, R. S. Orr, W. Schmidt-Parzefall, K. Winter, A. Brandt, F. W. Busser, G. Flugge and F. Niebergall *et al.*, *Nucl. Phys. B* **150** (1979) 221.
- [26] U. Amaldi and K. R. Schubert, *Nucl. Phys. B* **166** (1980) 301.
- [27] G. Antchev, P. Aspell, I. Atanassov, V. Avati, J. Baechler, V. Berardi, M. Berretti and E. Bossini *et al.*, *Europhys. Lett.* **96** (2011) 21002 [arXiv:1110.1395 [hep-ex]].